8-1-2022

Fabrication of porous extended-release tablets using dual nozzle fused deposition modeling 3D printing techniques

Sung-Chi Lee

FABRICATION OF POROUS EXTENDED-RELEASE TABLETS USING DUAL NOZZLE FUSED DEPOSITION MODELING 3D PRINTING TECHNIQUES

A Thesis Presented for the Master of Science Degree

The University of Mississippi

Sung-Chi Lee

August 2022

ABSTRACT

The aim of this study was to fabricate shell-core porous tablet formulations by fused deposition modeling dual nozzle three-dimensional printing coupled with hot-melt extrusion techniques. Acetaminophen was selected as the model drug for this study owing to its pH-independent property. The 3-point bend test and the stiffness test were performed to investigate the printability of filaments. The stiffness constant, *k*, was calculated to represent the printability by fitting the breaking distances and stress data into Hooke's law. The formulation 1 (F1) and formulation 2 (F2) filaments were printed successfully by demonstrating the preferred hardness with 16.74±3.55 and 14.72±2.20 respectively in *k* value (g/ mm^3). *In vitro* dissolution studies were performed in phosphate buffer (pH 6.8) to evaluate the drug release rate of the printed tablets. Due to SEM images, drug load, and other factors, F1 core tablets demonstrated a faster dissolution profile than F2 core tablets. Three different porous shells were designed to extend dissolution profiles by sealing the core tablet in it. From the result, both formulations with shell-core porous tablets demonstrated an extended dissolution profile in all designs. Therefore, a novel extended-release porous shell-core tablet was successfully developed, by altering the hole's quantity and location can acquire different dissolution profiles.

DEDICATION

This thesis is dedicated to everyone who helped me and guided me through my own times of stress and anxiety. Particularly thank my parents, Shun-Chien Lee and Hui-Ju Chan, who supported me so that I could conduct my project without worrying behind.

LIST OF ABBREVIATIONS AND SYMBOLS

ER	Extended-Release
APAP	Acetaminophen
PEO	Polyethylene Oxide
F	Formulation
HME	Hot-Melt Extrusion
3DP	Three-Dimensional Printing
FMD	Fused Deposition Modeling
DSC	Differential Scanning Calorimetry
FTIR	Fourier Transform Infrared
SEM	Scanning Electronic Microscopy

ACKNOWLEDGMENTS

I would like to express my deepest and most sincere thanks to my advisor, Dr. Michael A. Repka and my committee members, Dr. Eman Ashour and Dr. Suresh Bandari. I also want to thank two of my colleagues, Honghe Wang and Peilun Zhang, because I could not finish the whole project without assistance from them. In addition, I appreciate my department for allowing me to conduct my project.

Lastly, I would like to thank my family for their support and encouragement along the way.

TABLE OF CONTENTS

LIST OF TABLES

LIST OF FIGURES

CHAPTER 1

INTRODUCTION

The disease treatment depends on effective drug delivery systems to carry pharmaceutical ingredients (APIs) into humans. An effective drug delivery system requires certain APIs to be transported to a specific site at a controlled rate[1]. The oral drug delivery system is the most common, convenient, and acceptable route of administration among other drug delivery systems such as ocular, nasal, pulmonary, etc[2]. Water solubility is one of the basic requirements for oral administration of a drug. Inadequate dissolution and bioavailability reduction of a drug results from low aqueous solubility[3]. Owing to oral administration's convenience, patients relatively have high compliance with taking medicine *via* mouth. With different medicine descriptions, some drug is needed taking three times or even more times a day for immediate effect. For specific groups of people, they might need to take drugs which can extend the function of medicine to relief or prevent the symptom. There are some extended-release (ER) drugs have already produced on the market. For example, VoSpire ER, albuterol sulfate extended-release tablets, is a prescription medicine used to treat the symptoms of bronchospasm, acute or severe bronchospasm and exercise induced bronchospasm.

Hot-melt extrusion has been employed in industries since the 1930s[4]. At the beginning of the 1970s, HME was used in formulation development and product manufacturing in the pharmaceutical industry[4]. As a continuous process, HME pumps physical mixtures, APIs, and

other thermotolerant polymeric materials mixtures which pre-mixing without solvent or water, with rotating screws at the temperature above materials' glass transition temperature (Tg) or melting temperature (Tm) to conduct a molecular level mixing[4, 5]. These ingredients convert into an amorphous solid during the mixing process, which improves the oral bioavailability of poorly water-soluble drugs[6]. Currently, HME has been investigated by both academia and industry to improve poorly water-soluble APIs dissolution profile[7]. Compared with the traditional pharmaceutical manufacturing process, HME has fewer processing steps. It makes HME more efficient and convenient to fabricate a product without those downstream processes[7]. In a nutshell, the advantage of HME is a continuously reproducible process, fewer steps in manufacturing, solvent-free, water-free, and a wide range of API/polymer options[8].

HME has been used in numerous pharmaceutical applications. W.De, et al., 2015, evaluated polyvinyl alcohol (PVOH) polymers as a carrier for oral immediate-release (IR) dosage forms can optimize the release rate of poorly water-soluble drugs *via* HME[9]. A. Butreddy, et al., 2020, used polyethylene oxide (PEO) and gelling agents to fabricate an extended-release (ER) pellets by HME in order to utilize the abuse deterrence (AD) properties[10]. J.S. Koo, et al., 2019, successfully reduced the particle size of iron(II) sulfate ($FeSO_4$) from micron to nano size by dispersing $FeSO_4$ in the mixture (Span 80, Tween 80, and PEG 6000) by the HME process. Owing to the size reduction, the author found some advanced therapeutic potentials for colon cancer[11]. There are more applications that HME has widely employed such as sustained-release formulations[12], Taste-Masked tablets[2], chrono-modulated drug delivery systems[13], etc.

Three-dimensional printing (3DP) is a novel technology in recent. With computer-aided design (CAD) software, people can print any object through a 3D printer. The 3D printer has

been widely used in research, different types such as stereolithography apparatus (SLA)[14], selective laser sintering (SLS)[15, 16], laminated object manufacturing (LOM)[17], and fused filament fabrication (FFF), as known as fused deposition modeling (FDM)[18]. FDM is the most common and well-known technique which uses a thermoplastic material as a continuous filament in the pharmaceutical industry[19]. FDM is a nozzle-base deposition system that extrudes semi-molten filaments *via* a nozzle by depositing successively one horizontal plane at a time. The print head moved vertically to start a new layer after a layer finished[20]. FDM 3DP has advantages such as inexpensive manufacturing, the compatibility of using the thermotolerant pharmaceutical-grade polymers with APIs *via* HME and the ability to fabricate a new delivery system of drug[21]. Moreover, the 3DP technique can control every step at a time including design, manufacturing, and other changeable parameters to achieve fast, continuous and precise personal needs[22]. However, the accuracy and the quality of the dosage form *via* FDM fabrication are only supported by limited research.

In the traditional process, tablet manufacturers might face some problems such as large batches wasted, long production time, and expensive facilities[23]. Unlike the traditional pharmaceutical manufacture process, the combination of HME and 3DP is much more efficient and economical by reducing multiple processes which include milling, granulation, sieving, compressing, and coating[24, 25]. Moreover, this combination benefits pharmaceutical science by their advantages as followings: (1) improving the solubility and bioavailability of poorly water-soluble drugs; (2) the ability to fabricate tablets and other drug delivery systems; (3) the capability to produce complex structure dosages; (4) customized drug products[2, 7]. Furthermore, the combination of this technique has a potential that can be applied to develop a remote personalized healthcare system[26]. Some research put this idea as a primary incentive such as

personalization of dosing[23], customization of dosage forms[27], modification of drug release[21, 28, 29], adaptation of medicated devices[30, 31].

The aim of this study is to fabricate a novel and efficient method to manufacture porous tablets to extend the drug release by coupling HME and 3DP. A dual nozzle FDM 3D printer was utilized to achieve single-step production. By using dual nozzle 3DP, two filaments (shell formulation and core formulation) can be loaded separately and be printed simultaneously to achieve the purpose of integrated design.

CHAPTER 2

MATERIALS AND METHODS

Materials

Acetaminophen (APAP; Spectrum Chemical, New Brunswick, NJ, USA) was selected as a model API, Kollicoat®IR (BASF, Germany), Kollidon®VA 64 (BASF, Germany), Polyethylene Oxide (POLYOX™ WSR N10, USA), Polylactic acid (Ultimaker 2.85mm NFC PLA, Dutch), Potassium phosphate, monobasic, 99+%, ACS reagent (Thermo Scientific™, USA), Sodium hydroxide, 98.5%, pellets (Thermo Scientific™, USA)

Formulations

Three different formulations were developed (Table 1). Formulation 1 used 10% APAP mixing with 27% Kollidon®VA 64 and 63% Kollicoat®IR. Formulation 2 used 20% APAP mixing with 24% PEO N10 and 56% Kollicoat®IR. Formulation 3 used 20% APAP mixing with 24% Kollidon®VA 64 and 56% Kollicoat®IR. Three formulations were put into small bags and mixed by hand shaking for 5 minutes. The PLA was selected as shell filament.

Table 1. Composition of the formulations

Formulation	Drug (w/w)	Polymer (w/w)
F1	10%	27% Kollidon®VA 64, 63% Kollicoat®IR
F2	20%	24% PEO N10, 56% Kollicoat®IR
F3	20%	24% Kollidon®VA 64, 56% Kollicoat®IR

Preparation of Filaments by Using HME

In this study, hot melt extrusion was conducted to prepare 3D printing filament by using a parallel (11mm) twin-screw, co-rotating Pharma 11 Twin-screw Extruder (Process 11 Thermo Fisher Scientific, Waltham, DE, USA). Prior to processing, ingredients were weighted precisely, mixed properly, and manually loaded into the extruder during the process to keep a continuous loading. Physical mixtures were extruded at 140°C with the standard screw configuration (Thermo Fisher Scientific) with 3 mixing zones at 50 rpm screw speed. The extrudates were extruded by using a 2.5-mm round opening die. Following extrusion, these extrudates, as known as a filament, could be directly fed into the FDM 3D printer to print. F1 and F2 formulations were fabricated using the same printing parameters.

Tablet Design and Printing

Ultimaker 3 (Ultimaker B.V., Dutch, Fig. 1), a dual nozzle FDM 3D printer, was chosen to fabricate tablets. Core filaments of two formulations (Table 1) were manufactured *via* HME under the same process. Blender, a well-known 3D computer-aided design software, was conducted to fabricate three different porous structures (Fig. 2). All computer-aided designed

profiles were sent to Ultimaker Cura 4.13.1 which can adjust all printing process parameters on the 3D printer. The printing temperature was the only different parameter in the two printcore, others such as infill percentage, printing speed, layer height, and thickness were identical. PLA was printed at 200°C and both F1 and F2 were printed at 180°C.

By using dual nozzle 3DP, core and shell filaments were loaded into the hotend of the 3DP respectively at a time. PLA was loaded to print the shell structure *via* left printcore, and core filaments (F1 and F2) were loaded *via* right printcore. In this porous structure, all holes were designed in the same diameter and shape (circle). The tablet was designed with only small space on the sides, there are no spaces between the top and bottom (Fig. 3).

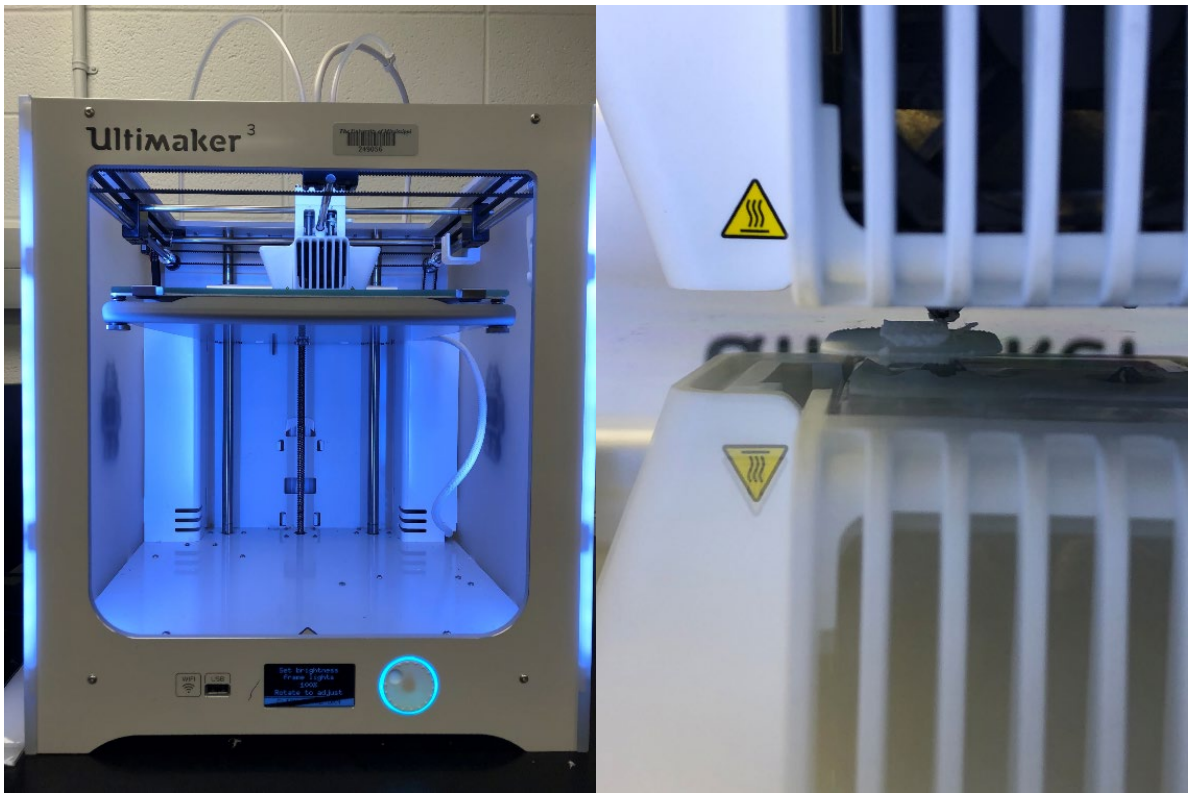

Fig. 1. The dual nozzle fused deposition modeling 3D printer. Left and right printcore can load different filaments at a time respectively, which means two materials can be printed on the same object.

Fig. 2. The different types of tablet design. a) Three holes on the top and bottom with six holes on the side. b) Seven holes on the top and bottom with twelve holes on the side. c) Only three holes on the top and bottom.

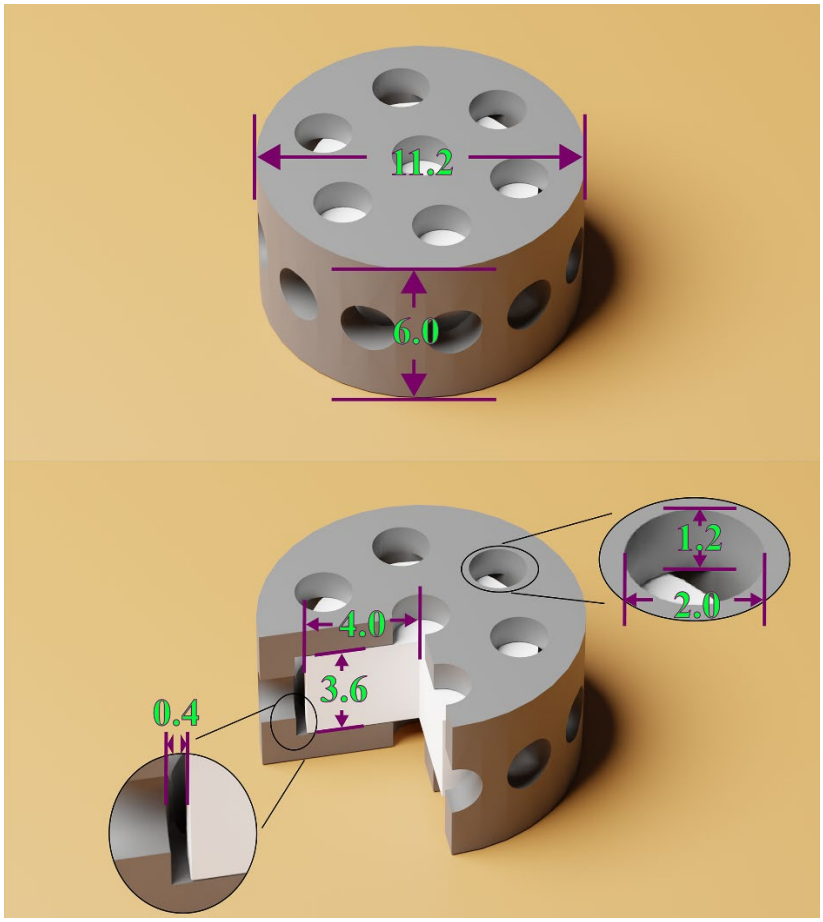

Fig. 3. The internal and external structure of the tablet. Use (b) in figure 2 as the demonstration. The core (white) is tightly bound with the shell's top and bottom. All holes are identical. Numbers unit in millimeter (mm).

Differential Scanning Calorimetry

A Differential scanning calorimetry (DSC) was conducted using TA Instruments (New Castle, DE, USA). Before testing, pure ingredients (physical mixtures) and milled filament were accurately weighted 5-8mg separately loaded into an aluminum-crimped pan and then sealed with a lid. After samples were well prepared, placed the samples on the testing zone. The testing was performed within the 25–250°C temperature range at a ramp rate of 20 °C/min. Nitrogen

was used as a purge at a flow rate of 50 mL/min. Data were collected and analyzed with TRIOS software.

In Vitro Dissolution Studies

A United States Pharmacopeia (USP) dissolution apparatus ll (Hanson SR8-plus™; Hanson Research, Chatsworth, CA, USA) was employed to perform the *in vitro* dissolution studies. Each experiment was assessed in triplicate and the temperature was set at 37.0 ± 0.5°C. Drug release occurred in 900 mL of pH 6.8 phosphate buffer and the paddle rotation speed was set at 50 rpm. Porous structure on the shell may cause tablets to float; therefore, sinkers were conducted to keep tablets submerged in the dissolution vessel[25]. F1 and F2 tablet samples were collected at 15, 30, 45, 60, 75, 90, 120, 180, 240, 300 min time points. Porous F1 tablet samples were collected at 0.25, 0.5, 0.75, 1, 1.5, 2, 3, 4, 5, 6, 8, 12, 24 hour time points. Porous F2 tablet samples were collected under the same time point with two extra time points (36 hours and 48 hours). All samples were diluted and analyzed using a UV-Vis spectrophotometer (Thermo Scientific™, GENESYS™ 180 UV-Vis Spectrophotometer) at 243 nm.

The Repka-Zhang Test

The Repka-Zhang method was employed to perform 3-point bend tests and stiffness tests in this study. The purpose of this method was to evaluate the printability of filaments[7]. A TA-XT2 analyzer (Texture Technologies Corp, New York, NY, USA) and the TA-95N probe set were used for the flexibility tests. The filament samples were cut into 6 cm length pieces. We used a 25mm width supporting gap to hold samples. The blade slowly moved down at speed of 10 mm/s till it reached 20 mm below where samples were placed. Each filament was repeated 12 times. The polylactic acid (PLA) filament was used as a reference material to compare the

difference between experimental designed filaments and marketing products. The data of breaking distance and loading force were recorded and analyzed using the Exponents software (Texture Technologies Corp. and Stable Micro Systems, Ltd., Hamilton, MA, USA).

For stiffness analysis, the experimental set up same as flexibility tests. The filament was cut into 6 cm size pieces and repeated 12 times as well. The only difference was that samples were placed on the flat solid surface, not on the supporting gap. The blade pressed samples directly with around 50% of filament diameter and breaking force data were recorded and analyzed using the Exponents software.

Fourier Transform Infrared Spectroscopy

An Agilent Cary 660 Fourier transform infrared spectroscopy spectrophotometer (Agilent Technologies, Santa Clara, CA, USA) was conducted to investigate interactions between the API and polymers over a 600-4000 cm^{-1} range. The FTIR spectra of the API, polymers, and finely milled extrudates were acquired respectively.

Scanning Electron Microscope

The surface morphology of the formulations was studied with a JSM-7200FLV Scanning Electron Microscope (JEOL, Peabody, MA, USA) with an accelerating voltage of 5 kV. All the samples were placed on the SEM stubs and adhered by using double-adhesive tape. The samples were sputter-coated with Platinum under an argon atmosphere using a fully automated Denton Desk V TSC Sputter Coater (Denton Vacuum, Moorestown, NJ, USA) prior to imaging.

CHAPTER 3

RESULTS AND DISCUSSION

Formulation

Kollicoat® IR, Kollidon® VA 64, and PEO N10 were selected in this study. Kollicoat® IR, a flexible grafted copolymer comprised of 25% polyethylene glycol and 75% polyvinyl alcohol (PEG-PVA), was developed first as a coating for immediate release drug. It has also been used as a hydrophilic pore former in the drug layering for sustained release tablet and peroxide-free binder[32, 33]. Kollidon® VA 64, a brittle and less flexible copolymer comprised of 60% of vinyl pyrrolidone and 40% vinyl acetate (PVP-PVAc). Pure Kollidon® VA 64 and Kollicoat® IR were not highly suitable for 3D printing; in other words, they were hard to extrude alone from the heated nozzle due to their properties. Solanki used Kollicoat® IR with Kollidon® VA 64 and HPMC as the plasticizers to optimize the extrusion conditions and make filament can be printed sussesfully[34]. PEO N10 was used to see the difference in results between Kollidon® VA 64. The viscosity of PEO N10 was higher than Kollidon® VA 64 which made filaments much more flexible and softer. F1 used API mixed only with Kollicoat® IR and Kollidon® VA 64, with no plasticizer was added. F2 changed Kollidon® VA 64 to PEO N10, no plasticizer added either. The reason both formylations can be extruded from the nozzle smoothly without any plasticizer was that the API (acetaminophen) acted like a plasticizer in this formulation. However, acetaminophen was not a real plasticizer that could make filament softer and more flexible,

increase its plasticity, and decrease its viscosity.

A shell-core design tablet has been developed for years. Tochukwu C. Okwuosa, et al., 2017, fabricated a delayed-release tablet by changing the shell thickness[29]. Small shell thickness differences could make a huge impact on drug release profiles. Jiaxiang Zhang, et al., 2021, produced a controlled release tablet by making a porous fast-release shell and a compact extended-release core[1]. In this study, the idea of the porous shell structure has been used. However, the difference between this porous shell structure with Zhang's was that all holes were designed in the same shape (circle) and size. Three different porous shells were designed (Fig. 3). Moreover, dual nozzle 3D printer was applied in this study which made the shell and core be printed together at a time. There were no spaces on the top and the bottom, only small spaces on the side (Fig 2).

With this porous shell structure, fluid flow can be easily controlled by porous size and quantity, even the position. Before F1 (10% API, 25% Kollidon®VA 64, 65% Kollicoat®IR) was chosen, 20% API was tested first (F3). The extrudate was too brittle and stiff to hold, it broke easily when it cooled down right after HME. In other words, F3 could not be printed. Owing to this, API was reduced to 10% and the extrudate turned out much more flexible. Like F1, F2 (20% API, 25% PEO N10, 55% Kollicoat®IR) was tested with 20% API first and the extrudate property was acceptable. F2 extrudates were flexible and can be bent and slightly twisted even they included with 20% API. Although 10% API did not be tested in F2, we could expect extrudates will be softer. The reason for this result could be caused by PEO N10 which can increase the filament's viscoelasticity.

Differential Scanning Calorimetry

As a thermoanalytical technique, DSC has been widely used to detect thermal transitions of polymeric materials. The DSC thermogram of APAP (Fig. 4) exhibited an endothermic melting peak at 172°C. As expected, the APAP peak was absent after the 3DP process. This demonstrated that APAP could disperse or dissolve into the molten polymer matrix during the HME process. It also indicated this HME process formed an amorphous solid dispersion.

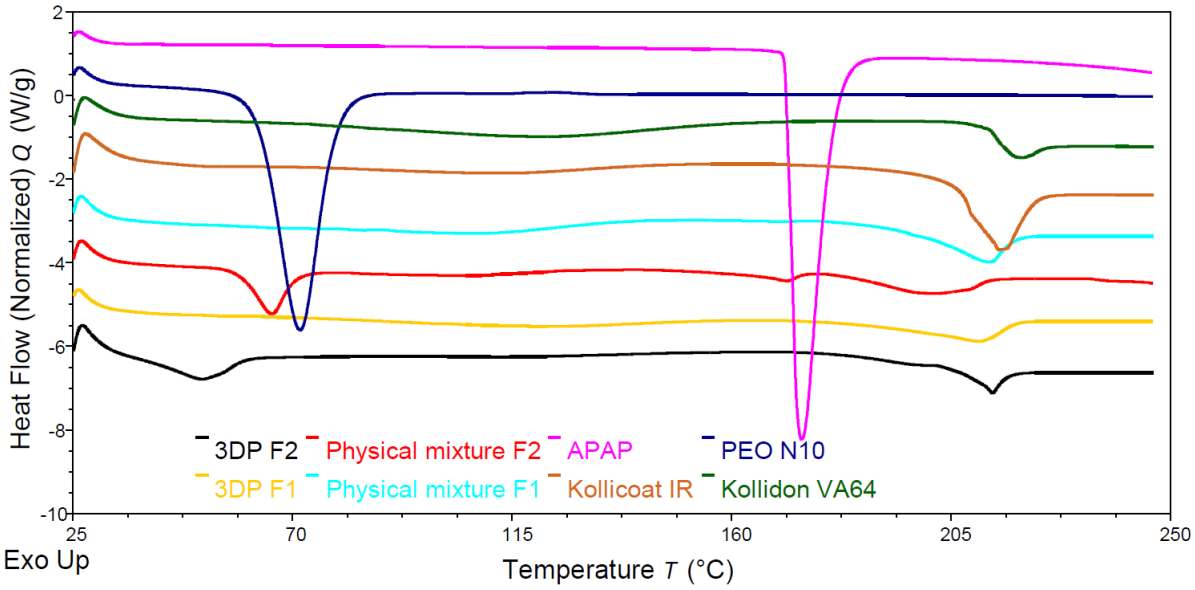

Fig. 4. DSC thermogram of acetaminophen, PEO N10, Kollidon®VA 64, Kollicoat®IR and formulation 1 and formulation 2.

In Vitro Drug Release Study

Acetaminophen (APAP), a neutral substance, does not ionize unless the pH is over 8. Unlike weak acid and weak base, drugs have a preferred location in absorption, neutral drugs are absorbed from both the stomach and the intestine. Furthermore, the neutral characteristic makes APAP be a pH-independent drug. In this study, APAP was chosen as API in formulations due to its pH-independent property. Pure core tablets (no shell) were printed first to get the drug release

profile in pH (Fig. 5). F1 reached 80% drug release at 60 min and after around 120 mins all tablets were dissolved. F2 reached 80% drug release at 120 min and dissolved completely after 210 min.

Dissolution profiles of FDM 3D-printed porous tablets with different numbers of holes in pH 6.8 media were listed in Fig. 6. The drug release pattern was affected by holes on the shell. As expected, porous tablets with six holes had the slowest dissolution profile. The inner core was designed tightly connecting with the shell on the top and the bottom. Due to the limited surface area exposed, fluid was hard to get into the core through holes and made drugs hard to release from the core. However, tablets with twelve holes and twenty-six holes had relatively faster dissolution profiles because they both had holes on the side. Tablets with holes on sides could increase the speed of drug release. Although the core was tightly connected to the shell, it had 0.4 mm spaces on the side (Fig. 3). Owing to this space, fluid could easily get into tablets through side holes and made the core dissolve faster.

From the drug release pattern (Fig. 6), F1 tablets reached around 10%, 30%, and 85% in three different holes respectively after five hours; F2 tablets reached around 15%, 42%, and 80% in three different holes respectively after twelve hours. Moreover, the fastest fully dissolving time in F1 tablets was about twelve hours and forty-eight hours in F2 tablets. This was longer than pure core in two formulations achieved complete drug release in about 120 min and 210 min in F1 and F2 respectively. For this design, not only numbers of hole affected dissolution profiles but locations (top/bottom or side). From the dissolution profile result, the drug release pattern was successfully extended. The more holes on the shell, the shorter time it took to fully dissolved. In other words, specific drug release profiles could be acquired by designing different porous shell structures.

In addition, one of the reasons the F1 tablets could get a faster drug release profile was the drug load. Under the same tablet weight and size, F1 had a 10% drug load, and F2 had 20%.

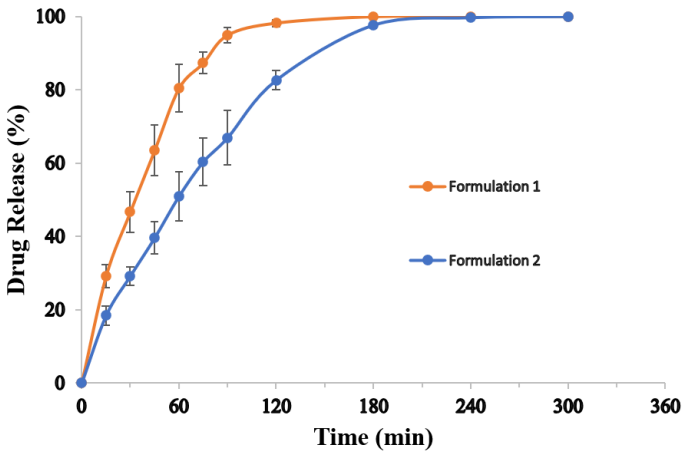

Fig. 5 Pure core tablets without shell covering drug release profile.

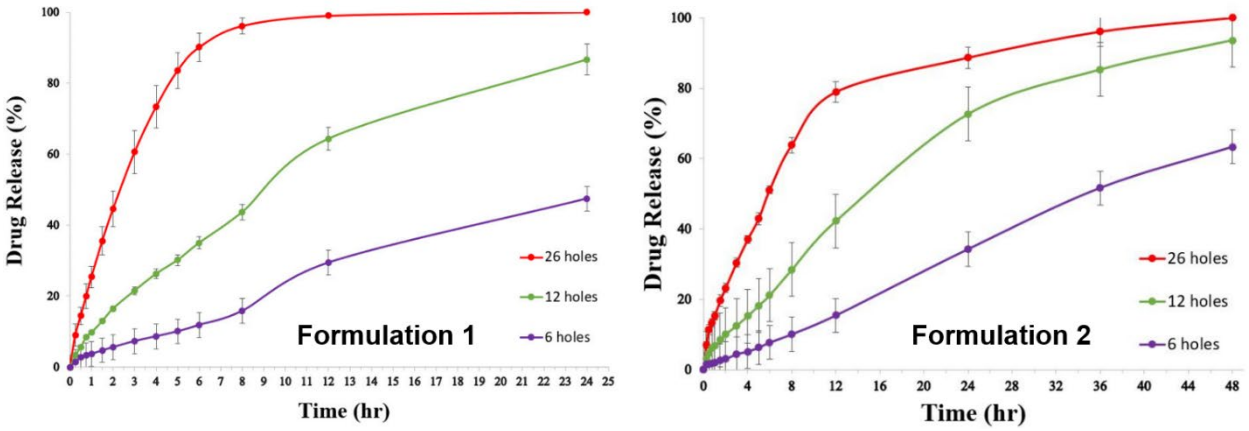

Fig. 6. The drug release profile of shell-core porous tablets in three different amounts of the hole.

The Repka-Zhang Test

The 3D printing process highly relied on filament's property. The filament's printability was affected by softness and brittleness. Nozzles extruded materials continuously by feeding

filaments through gears. Soft filaments were easily squeezed by gears which caused the printing process discontinuous, and hard to load into the 3D printer because of low abrasion resistance. Owing to this, soft filaments were hardly imported by gears and often blocked the nozzle. Similarly, brittle filaments were broken into two pieces by gears once put into the 3D printer. The 3-point bend test was used to determine the breaking force, breaking distance, and breaking stress of filaments (Table 2). Breaking stress was the maximum force that applied to a cross sectional area of the filament:

$$\sigma \text{ (Breaking stress)} = \text{Force} / \text{Area}$$

In this study, filaments were extruded via a 2.5 mm diameter die, but the PLA used for commercial reference filament in 3D printing had a 2.65 mm diameter. Therefore, comparing filaments breaking stress with each other was meaningful and reasonable rather than breaking force. The harder texture of filaments would result in higher breaking stress. Moreover, filaments with softer textures brought about longer breaking distances. Based on the stress-strain behavior, polymers with high stress or low strain (short breaking distance) indicated polymers were brittle. Table 2 presented that the breaking distance of similar formulation (F1 and F3) filaments was higher than PLA (6.00 ± 0.25 mm) while the stress in both filaments were less than PLA (119.028±7.39). F2 had a lower breaking distance and stress than PLA. Thus, brittleness was not considered. However, whether a filament was suitable for printing or not, reasons depend not only on the relationship between the stress and breaking but also on other factors. Therefore, Hooke's law was applied to assist in evaluating the printability of filaments:

$$F = -kx$$

F represented the stress when the bend point moved away from the center to distance x, and the negative sign means the whole movement was away from the center. From the 3-point bend

test figure (Fig. 7), when the sample filament was placed on the supporting gap (start), it can be seen as the elastic region (straight line). The bending curve was indicated the plastic region. A sample filament had elasticity only when it was in an elastic state (when it was bending not breaking), and when the force was removed, the filament will return to its starting state. This was very similar to stretching a spring. Owing to this, Hooke's law can be used to investigate the printability of filaments.

The maximum force on the breaking point was recorded (Fig. 7). The stiffness constant "k" was calculated from the data above. When stiffness constant reached a specific value, it represented the extrudates could be printed. However, the k value was influenced by the extrudate's physical properties. In this study, F1 and F3 used the same material but in different ratios. Although F1 and F3 seems had similar data in Table 2, F3 failed in collecting filaments from the HME process which cannot be printed. Therefore, the stiffness test was applied to investigate more details. The F3 data were collected from broken pieces. Due to this, F1 decreased by10% in API and increased by 3% in Kollidon®VA 64, and by 7% in Kollicoat®IR. From the stiffness test, F1 had double force and stress value compared to F3 (Table 3). The increased stiffness utilized F1 filaments can be collected which did not break right during the HME process. Thus, it can be conducted in the 3D printing process after HME.

Furthermore, F2 had lower stress and stiffness constant than F3. API and Kollicoat®IR percentages were the same in both F2 and F3, the only difference was F2 mixed with PEO N10 and F3 mixed with Kollidon®VA 64 respectively. F2 with low stiffness did not mean it was brittle. On the contrary, it was flexible (soft). The F2 filament was similar to the reference PLA filament when it was extruded from HME. However, not only low force was observed in the 3-point bend test but stiffness test. The feature of low stiffness with flexibility in F2 was attributed

to the PEO N10. PEO was used as the binder which had high viscosity and wide pH stability. The viscoelastic can reduce drifting, misting, and splattering in granulation. Owing to this, PEO was used to increase the flexibility of filament in 3D printing.

Table 2. The 3-point bend test of the filaments (Mean ± SD, n = 12)

Formulation	Force	Stress	Distance	*k*	Printability
PLA	4272.38±105.32	670.056±16.52	6±0.25	111.75±2.51	YES
F1	588.83±73.74	110.96±13.90	11.4±1.28	16.74±3.55	YES
F2	448.22±33.29	122.20±14.63	9.87±1.51	14.72±2.2	YES
F3	301.97±33.03	56.90±6.22	4.93±0.21	11.54±1.27	NO

Parameters: force (g), stress (g/mm^2), distance (mm), "k" value (g/mm^3), and result of filament printability

Table 3. The stiffness test of the filaments (Mean ± SD, n = 12)

Formulation	Force (g)	Stress (g/mm^2)	Deformation (mm)
PLA	36399.32±374.19	5914.36±60.80	1.4
F1	10681.47±379.22	2012.86±71.46	1.3
F2	4174.30±852.14	702.03±188.46	1.2
F3	5006.70±392.13	1317.76±103.21	1.1

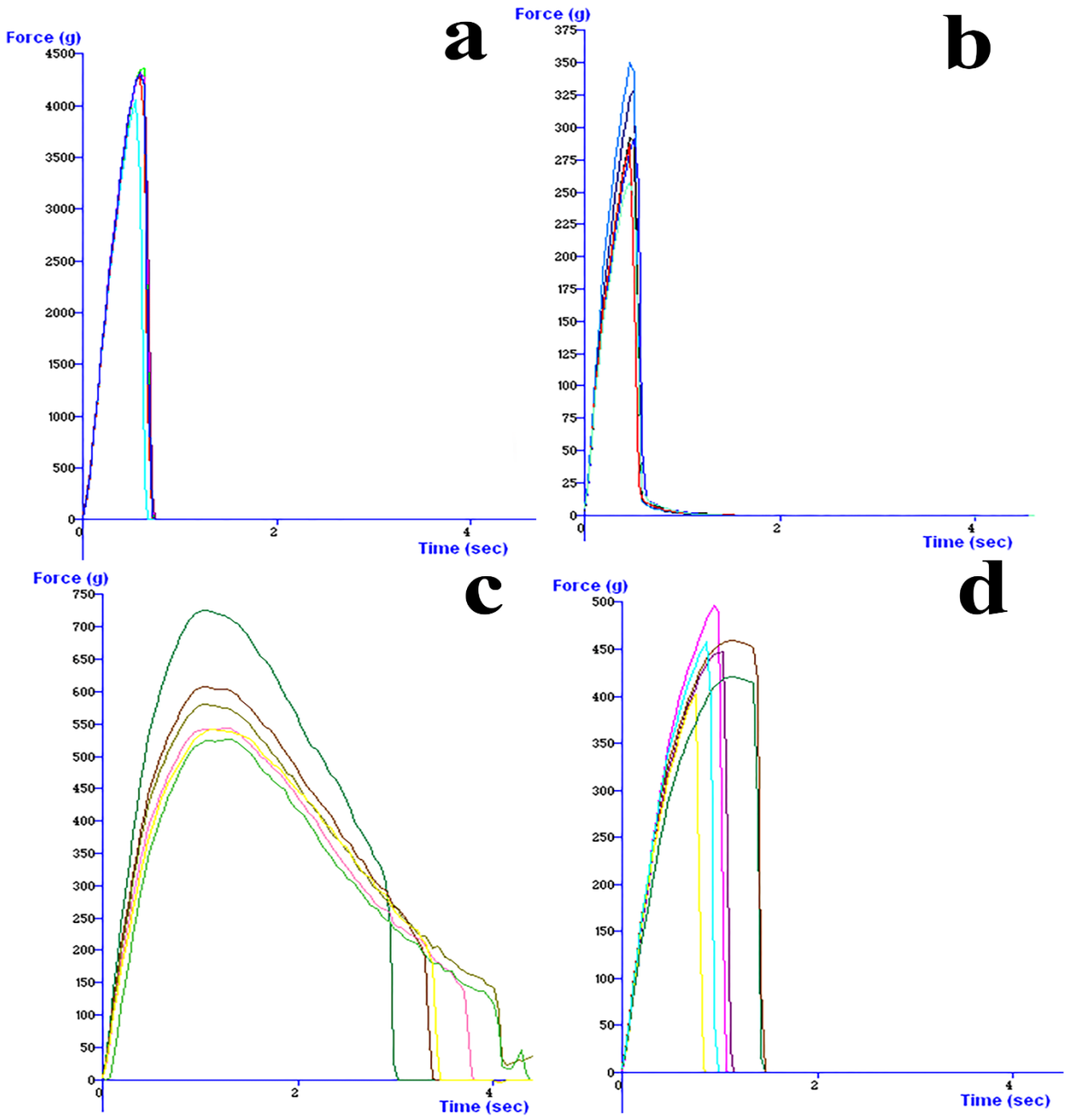

Fig. 7. The force-time curve of the 3-point bend test of the filaments. a) PLA. b) Formulation 3. c) Formulation 1. d) Formulation 2.

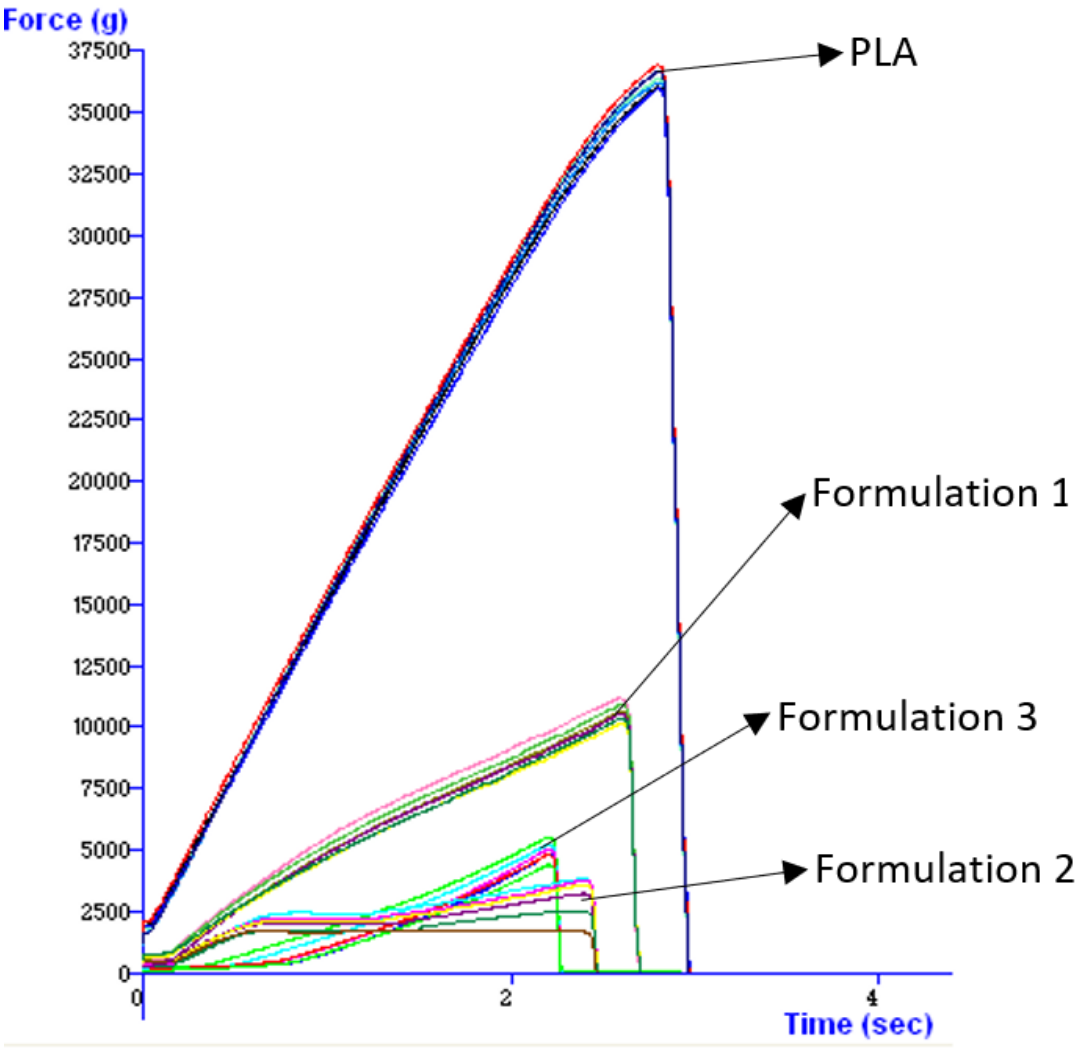

Fig. 8. The force-time curve of the stiffness test of the filaments.

Fourier Transform Infrared Spectroscopy

FTIR was carried out to determine possible interactions between the drugs and the rest of the substances in extrudates (Fig. 9). The wide peak around 3300 cm^{-1} was assigned to O-H stretching in the hydroxyl group of Kollicoat®IR and PEO. The peak around 2900 cm^{-1} was attributed to C-H stretching vibration in an alkane of Kollicoat®IR, Kollidon®VA 64, and PEO. The sharp peak showed at 1100 cm^{-1} due to C-O stretching in the hydroxyl group of

Kollicoat®IR, Kollidon®VA 64, and PEO. In addition, the peak at 1200 cm^{-1} was assigned to C-O-C stretching in the alkyl ether of Kollicoat®IR and Kollidon®VA 64. Kollidon®VA 64, Kollicoat®IR, and PEO showed an absorbance peak around 1700 cm^{-1} which can be represented as C=O stretching or O-C=O functional group. This peak slightly shifted in F1, indicating the carbonyl group (proton acceptor group) in each of them had an interaction with the hydroxyl group (proton donor group), including forming the intermolecular hydrogen bond. In F2 this peak shifted more than in F1 which means this interaction was stronger in F2.

From the acetaminophen spectra, the peak showed at 1500-1600 cm^{-1} peak that C-N-C=O stretching and N-H bend in secondary amide. The 950-1200 cm^{-1} peak was assigned to aromatic C-H in-plane bend and 800-850 cm^{-1} was attributed to aromatic C-H out-of-plane bend. The peak at 1200-1450 cm^{-1} was caused by O-H (alcohol) in-plane bend. During the HME process, APAP was dispersed into the polymer matrix. Owing to the temperature, the crystal structure transformed into an amorphous form. Moreover, the peak at around 3200-3400 cm^{-1} did not shift to a lower wavenumber. This indicated the O-H structure on phenol did not form a hydrogen bond with the hydroxyl group.

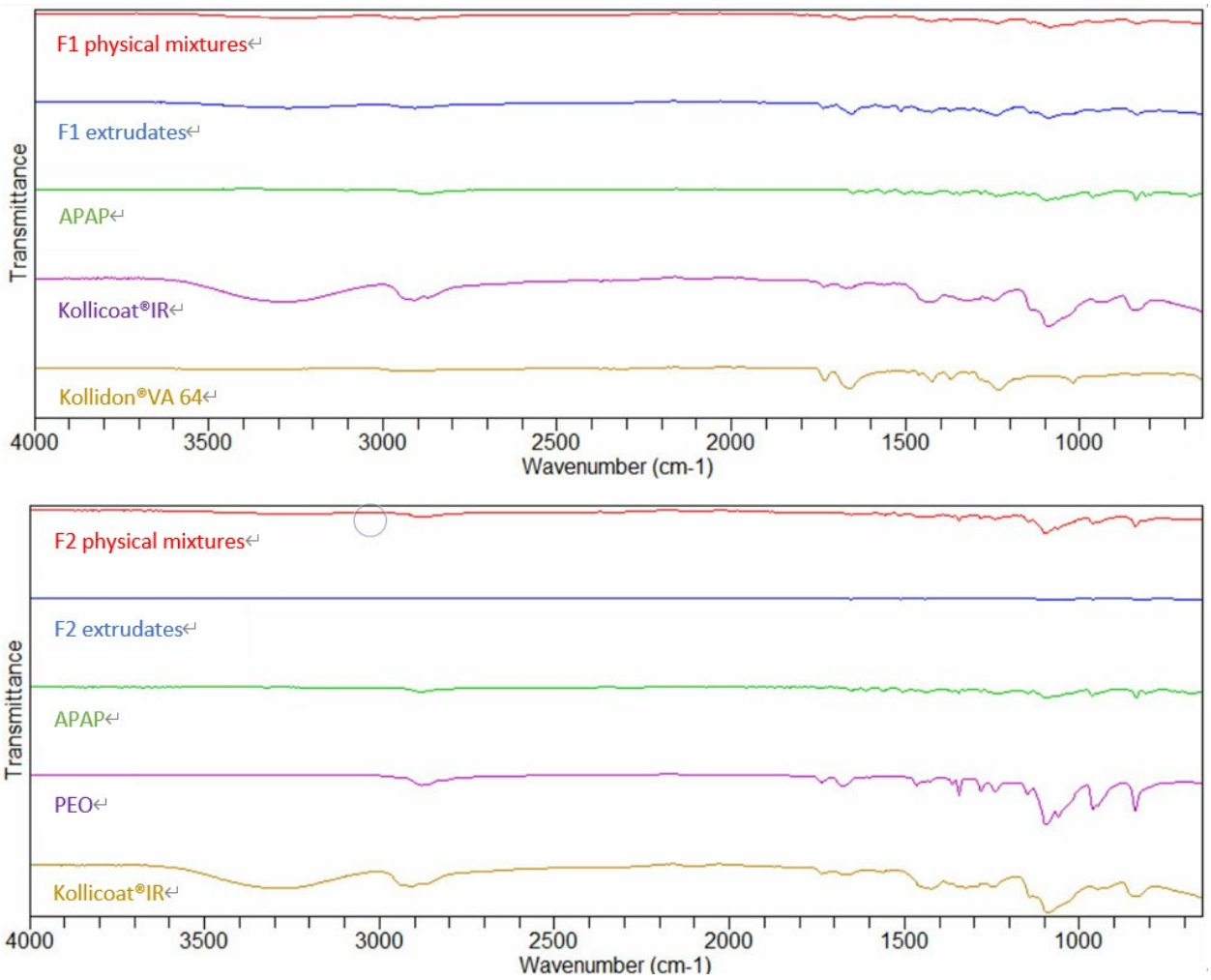

Fig. 9. The FTIR spectra of substances and extrudates in two formulations.

Scanning Electron Microscope

SEM images of core and shell surface structures have been investigated (Fig. 10). PLA was selected to use as the shell material. From figure 10, the PLA shell showed a sealed, smooth surface without any holes or cracks on it. This represented no fluid could penetrate or flow into the core through the shell itself. Where the fluid could cross the shell was controlled by the location of opening holes on the shell.

The F1 core image showed that the surface was uneven with small cracks, this result might

be caused by Kollidon® VA64. The property of Kollidon® VA64 after HME was mentioned (brittle and less flexible). Even though the F1 filament can be printed because APAP plasticized two polymers, from the SEM image it had no smooth surface. Because this 3D printing technique prints objects layer-by-layer, the previous layer might be dragged or damaged by processing the next layer when extrudates had not enough softness. However, F2 replaced Kollidon® VA64 with PEO and this made filaments and extrudates more flexible and much softer. Again, from figure 10, surfaces on the F2 tablets were smoother and flatter than F1's. Those little holes were caused by filament discontinuously pushing through the gear when the nozzle changed the direction to print another line. All tablet's infill density was set as 100% thus surface property was the only thing that could be considered in SEM. These small cracks on the F1 core could let fluid get into the tablet much easier than the F2 core, this might be one of the reasons that caused F1 to have a faster dissolution profile.

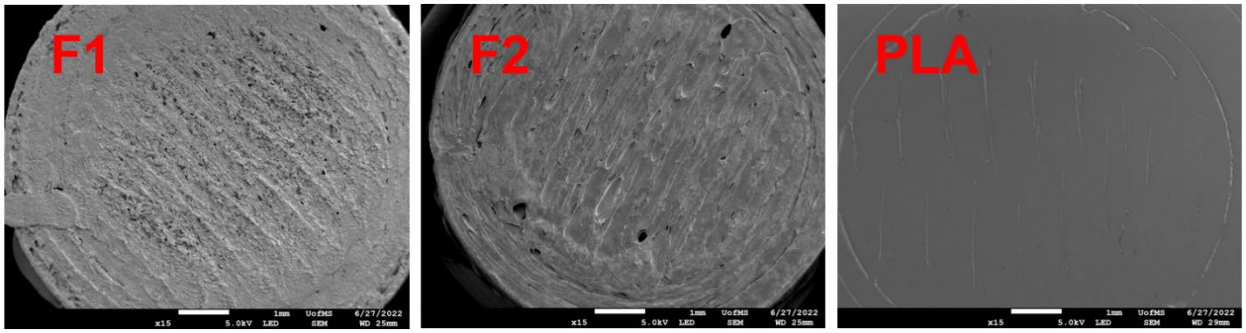

Fig. 10. SEM images of shell and core at 15 magnification levels.

Drug Content Study

For F1 and F2 these two formulations, the temperature of the HME and 3D printing was 140°C and 180°C. Two formulation filaments and 3D-printed tablets had a theoretical drug amount witch between 99-102% (Table 4). It indicated there was no significant difference in

drug contents before or after the 3D printing process. However, acetaminophen can be seen as a good thermal stability API during HME and 3D printing because the degradation temperature is over 200°C.

Table 4. Drug Content of Filaments and Tablets of Formulations 1 and 2 (Mean ± SD, n = 6

Formulation	Filament (%)	Tablet (%)
F1	101.33±0.34	102.75±0.91
F2	99.28±0.65	101.46±1.06

CHAPTER 4

CONCLUSION

In this study, a novel extended-release porous shell-core tablet was successfully developed via dual nozzle fused deposition modeling 3D printing paired with hot-melt extrusion techniques. Extrudates (filaments) were different in properties, especially when the composition was not alike. Three-point bend test was performed, and the results were applied to Hooke's Law which could assist to express the relationship between the hardness of filaments with data. The stiffness test was conducted to evaluate more details in formulations when composition was not suitable using Hooke's Law. Dissolution profiles showed hole's quantity and location affected drug release, depending on the number of pores and location. Pure F1 and F2 tablets reached full drug release at around 120 min and 210 min. Both formulations were extended in drug release when porous-designed shells were applied to core tablets. By altering holes on the shell, a wide range of drug release profiles can be fulfilled in different demands. As 3D printing techniques advance, many structures have been designed to meet customers' needs. However, the industrial production of pairing FDM 3DP with HME techniques is still challenging. Once this combination becomes more well-developed, customizing treatment would turn into a target with potential for development.

BIBLIOGRAPH

1. Zhang, J.; Xu, P.; Vo, A. Q.; Repka, M. A., Oral drug delivery systems using core-shell structure additive manufacturing technologies: a proof-of-concept study. J Pharm Pharmacol 2021, 73 (2), 152-160.
2. Wang, H.; Dumpa, N.; Bandari, S.; Durig, T.; Repka, M. A., Fabrication of Taste-Masked Donut-Shaped Tablets Via Fused Filament Fabrication 3D Printing Paired with Hot-Melt Extrusion Techniques. AAPS PharmSciTech 2020, 21 (7), 243.
3. Kim, D. S.; Cho, J. H.; Park, J. H.; Kim, J. S.; Song, E. S.; Kwon, J.; Giri, B. R.; Jin, S. G.; Kim, K. S.; Choi, H. G.; Kim, D. W., Self-microemulsifying drug delivery system (SMEDDS) for improved oral delivery and photostability of methotrexate. Int J Nanomedicine 2019, 14, 4949-4960.
4. Patil, H.; Tiwari, R. V.; Repka, M. A., Hot-Melt Extrusion: from Theory to Application in Pharmaceutical Formulation. AAPS PharmSciTech 2016, 17 (1), 20-42.
5. Liu, C.; Liu, Z.; Chen, Y.; Chen, Z.; Chen, H.; Pui, Y.; Qian, F., Oral bioavailability enhancement of beta-lapachone, a poorly soluble fast crystallizer, by cocrystal, amorphous solid dispersion, and crystalline solid dispersion. Eur J Pharm Biopharm 2018, 124, 73-81.
6. Zhang, J.; Xu, P.; Vo, A. Q.; Bandari, S.; Yang, F.; Durig, T.; Repka, M. A., Development and evaluation of pharmaceutical 3D printability for hot melt extruded cellulose-based filaments. J Drug Deliv Sci Technol 2019, 52, 292-302.
7. Lang, B.; McGinity, J. W.; Williams, R. O., 3rd, Hot-melt extrusion--basic principles and pharmaceutical applications. Drug Dev Ind Pharm 2014, 40 (9), 1133-55.

8. De Jaeghere, W.; De Beer, T.; Van Bocxlaer, J.; Remon, J. P.; Vervaet, C., Hot-melt extrusion of polyvinyl alcohol for oral immediate release applications. Int J Pharm 2015, 492 (1-2), 1-9.
9. Butreddy, A.; Sarabu, S.; Dumpa, N.; Bandari, S.; Repka, M. A., Extended-release pellets prepared by hot melt extrusion technique for abuse deterrent potential: Category-1 in-vitro evaluation. Int J Pharm 2020, 587, 119624.
10. Koo, J. S.; Lee, S. Y.; Azad, M. O. K.; Kim, M.; Hwang, S. J.; Nam, S.; Kim, S.; Chae, B. J.; Kang, W. S.; Cho, H. J., Development of iron(II) sulfate nanoparticles produced by hot-melt extrusion and their therapeutic potentials for colon cancer. Int J Pharm 2019, 558, 388-395.
11. Islam, M. T.; Maniruzzaman, M.; Halsey, S. A.; Chowdhry, B. Z.; Douroumis, D., Development of sustained-release formulations processed by hot-melt extrusion by using a quality-by-design approach. Drug Deliv Transl Res 2014, 4 (4), 377-87.
12. Dumpa, N. R.; Sarabu, S.; Bandari, S.; Zhang, F.; Repka, M. A., Chronotherapeutic Drug Delivery of Ketoprofen and Ibuprofen for Improved Treatment of Early Morning Stiffness in Arthritis Using Hot-Melt Extrusion Technology. AAPS PharmSciTech 2018, 19 (6), 2700-2709.
13. Xu, L.; Yang, Q.; Qiang, W.; Li, H.; Zhong, W.; Pan, S.; Yang, G., Hydrophilic Excipient Independent Drug Release from SLA-Printed Pellets. Pharmaceutics 2021, 13 (10).
14. Fina, F.; Goyanes, A.; Gaisford, S.; Basit, A. W., Selective laser sintering (SLS) 3D printing of medicines. Int J Pharm 2017, 529 (1-2), 285-293.
15. Kulinowski, P.; Malczewski, P.; Pesta, E.; Łaszcz, M.; Mendyk, A.; Polak, S.; Dorożyński, P., Selective laser sintering (SLS) technique for pharmaceutical applications—Development

of high dose-controlled release printlets. Additive Manufacturing 2021, 38.

16. Chang, B.; Parandoush, P.; Li, X.; Ruan, S.; Shen, C.; Behnagh, R. A.; Liu, Y.; Lin, D., Ultrafast printing of continuous fiber-reinforced thermoplastic composites with ultrahigh mechanical performance by ultrasonic-assisted laminated object manufacturing. Polymer Composites 2020, 41 (11), 4706-4715.
17. Arafat, B.; Qinna, N.; Cieszynska, M.; Forbes, R. T.; Alhnan, M. A., Tailored on demand anti-coagulant dosing: An in vitro and in vivo evaluation of 3D printed purpose-designed oral dosage forms. Eur J Pharm Biopharm 2018, 128, 282-289.
18. Peng, W.; Datta, P.; Ayan, B.; Ozbolat, V.; Sosnoski, D.; Ozbolat, I. T., 3D bioprinting for drug discovery and development in pharmaceutics. Acta Biomater 2017, 57, 26-46.
19. Aumnate, C.; Pongwisuthiruchte, A.; Pattananuwat, P.; Potiyaraj, P., Fabrication of ABS/Graphene Oxide Composite Filament for Fused Filament Fabrication (FFF) 3D Printing. Advances in Materials Science and Engineering 2018, 2018, 1-9.
20. Chai, X.; Chai, H.; Wang, X.; Yang, J.; Li, J.; Zhao, Y.; Cai, W.; Tao, T.; Xiang, X., Fused Deposition Modeling (FDM) 3D Printed Tablets for Intragastric Floating Delivery of Domperidone. Sci Rep 2017, 7 (1), 2829.
21. Goole, J.; Amighi, K., 3D printing in pharmaceutics: A new tool for designing customized drug delivery systems. Int J Pharm 2016, 499 (1-2), 376-394.
22. Skowyra, J.; Pietrzak, K.; Alhnan, M. A., Fabrication of extended-release patient-tailored prednisolone tablets via fused deposition modelling (FDM) 3D printing. Eur J Pharm Sci 2015, 68, 11-7.
23. Zhang, J.; Feng, X.; Patil, H.; Tiwari, R. V.; Repka, M. A., Coupling 3D printing with hot melt extrusion to produce controlled-release tablets. Int J Pharm 2017, 519 (1-2), 186-197.

24. Zhang, J.; Yang, W.; Vo, A. Q.; Feng, X.; Ye, X.; Kim, D. W.; Repka, M. A., Hydroxypropyl methylcellulose-based controlled release dosage by melt extrusion and 3D printing: Structure and drug release correlation. Carbohydr Polym 2017, 177, 49-57.
25. Awad, A.; Trenfield, S. J.; Gaisford, S.; Basit, A. W., 3D printed medicines: A new branch of digital healthcare. Int J Pharm 2018, 548 (1), 586-596.
26. Beck, R. C. R.; Chaves, P. S.; Goyanes, A.; Vukosavljevic, B.; Buanz, A.; Windbergs, M.; Basit, A. W.; Gaisford, S., 3D printed tablets loaded with polymeric nanocapsules: An innovative approach to produce customized drug delivery systems. Int J Pharm 2017, 528 (1-2), 268-279.
27. Arafat, B.; Wojsz, M.; Isreb, A.; Forbes, R. T.; Isreb, M.; Ahmed, W.; Arafat, T.; Alhnan, M. A., Tablet fragmentation without a disintegrant: A novel design approach for accelerating disintegration and drug release from 3D printed cellulosic tablets. Eur J Pharm Sci 2018, 118, 191-199.
28. Okwuosa, T. C.; Pereira, B. C.; Arafat, B.; Cieszynska, M.; Isreb, A.; Alhnan, M. A., Fabricating a Shell-Core Delayed Release Tablet Using Dual FDM 3D Printing for Patient-Centred Therapy. Pharm Res 2017, 34 (2), 427-437.
29. Fu, J.; Yu, X.; Jin, Y., 3D printing of vaginal rings with personalized shapes for controlled release of progesterone. Int J Pharm 2018, 539 (1-2), 75-82.
30. Muwaffak, Z.; Goyanes, A.; Clark, V.; Basit, A. W.; Hilton, S. T.; Gaisford, S., Patient specific 3D scanned, and 3D printed antimicrobial polycaprolactone wound dressings. Int J Pharm 2017, 527 (1-2), 161-170.
31. Ali, S., Kollicoat® IR: Minimizing the Risks for Oxidative Degradation of Drugs. Journal of Analytical & Pharmaceutical Research 2016, 2 (3).

32. Siepmann, F.; Hoffmann, A.; Leclercq, B.; Carlin, B.; Siepmann, J., How to adjust desired drug release patterns from ethylcellulose-coated dosage forms. J Control Release 2007, 119 (2), 182-9.

33. Solanki, N. G.; Tahsin, M.; Shah, A. V.; Serajuddin, A. T. M., Formulation of 3D Printed Tablet for Rapid Drug Release by Fused Deposition Modeling: Screening Polymers for Drug Release, Drug-Polymer Miscibility and Printability. J Pharm Sci 2018, 107 (1), 390-401.

VITA

SUNG-CHI LEE

kennylee0001@gmail.com

MILITARY SERVICE

Substitute Military Service at Hualien County Fire Department, Hualien Branch, June 2015

EDUCATION

M.S., Pharmaceutics, University of Mississippi, August 2022

Thesis: Fabrication of Porous Extended-Release Tablet Using Dual Nozzle Fused Deposition Modeling 3D Printing Techniques

B.S., Medical Applied Chemistry, Chung Shan Medical University, June 2015